# Gyrokinetic simulation tests of quasilinear and tracer transport

R. E. Waltz,[1,a)] A. Casati,[2] and G. M. Staebler[1]
[1]*General Atomics, P.O. Box 85608, San Diego, California 92186-5608, USA*
[2]*CEA-Cadarache, IRFM, F-13108 St-Paul lez Durance, France*

(Received 24 March 2009; accepted 8 June 2009; published online 13 July 2009)

A nonlinear gyrokinetic simulation code is used to test the *quasilinear transport approximation* (QLTA) with simulated nonlinear spectral (potential field) intensity. Two common forms of the QLTA are defined. The first uses the linear *mode spectrum* (mQLTA) and the second uses the complete *frequency spectrum* (fQLTA) for the nonlinear spectral intensity. The mQLTA is tested via two-step linear then nonlinear simulations convoluting a *quasilinear weight* with a nonlinear field intensity *spectral weight* to get the quasilinear transport in comparison with the actual nonlinear transport. The fQLTA is tested via one-step simulations that have ion and electron "plasma species" at full densities and "tracer species" at negligible densities (and making no contribution to the Poisson field solve equation). If the tracer and plasma gyrokinetic equations are identical, then so are their respective energy and particle diffusivities. Comparing tracer and plasma (actual) diffusivities, when the tracer equation nonlinearity is deleted, provides a quantifiable test of the fQLTA form. The mQLTA preserves ambipolarity but the two-step test includes only the leading linear normal modes at each wave number. The one-step test of the fQLTA subsumes all normal modes but precludes ambipolar particle flow. The mQLTA and fQLTA quasilinear weights (per normal mode) are shown to be identical for a commonly used (but unphysical) mode frequency line width model. In successful cases, quasilinear diffusivities are typically 1.4–1.8 (1.2–1.4) larger than actual diffusivities for mQLTA (fQLTA). The QLTA is expected to make best predictions in the ratios of energy and particle flows. Electron to ion energy flow ratios are well approximated but both forms of the QLTA appear to breakdown most evidently for ratios of particle to energy flows in cases with strongly pinched (and impractically large) particle flows. An example of the so-called *passive tracer diffusivity*, which includes only linear and nonlinear $E\times B$ motion, is given for comparison with actual diffusivities. © *2009 American Institute of Physics*. [DOI: 10.1063/1.3167391]

## I. INTRODUCTION AND SUMMARY

The *quasilinear transport approximation* (QLTA) has a long history in plasma physics, which we do not attempt to disentangle here for the lack of a general definition and context. In the present context of radially local turbulent transport flows in toroidal and magnetically confined plasmas such as tokamaks, there are two commonly defined forms of the QLTA. Each seeks to approximate the time and flux surface average transport flows by convolving a *quasilinear weight* with a (potential field intensity) *spectral weight* per wave number (i.e., toroidal $n$-number). As the name implies the quasilinear weight is derived from the *linear* correlation of the density (or energy) perturbations and (in the case of electrostatic transport) the radial $E\times B$ velocity perturbations. The spectral weight captures the saturated strength of the turbulence, which depends on the *nonlinear* coupling of the wave numbers. If the quasilinear weight convolution per wave number with the spectral weight is further broken into a *linear normal mode spectrum*, we refer to the "mode" QLTA (or mQLTA). If broken into a general *frequency spectrum*, we refer to the "frequency" QLTA (or fQLTA). The textbook definitions of quasilinear transport in Refs. 1 and 2 correspond to mQLTA and fQLTA, respectively. The reader may consult these for appropriate historical references.

The mQLTA is a crucial ingredient in the construction of physically comprehensive theory based transport models like MMM95,[3] GLF23,[4] TGLF,[5] or QualiKiz[6] and is of great practical interest. In these models the quasilinear weight is obtained from the linear normal mode dispersion relation following from the dynamical (fluid, gyrofluid, or gyrokinetic) equations and the Poisson (or quasineutrality) field solve equations. The spectral weight is given by a nonlinear saturation (or mixing length) rule (or model) involving the linear growth rate. The most important and powerful feature of the mQLTA is the prediction that the ratio of the plasma particle flow (as well as impurity, momentum, turbulent energy exchange, energetic particle, or electron energy flows) to ion energy flow (per wave number) is expected to follow from the ratio of the quasilinear weights in the respective channels independent of the model for the spectral weight, i.e., each transport channel uses the same spectral weight. Furthermore using the mQLTA, particle flows are guaranteed to be ambipolar since quasineutrality is built into the normal mode dispersion relation. A testable corollary of the (successful mQLTA is that the statistically dominant nonlinear cross-phase angle for fluctuations in density and temperature with respect to the potential (or with each other) should be accurately given by the linear normal mode cross-phase angles. A similar statement can be made for the relative sizes of the fluctuations.

a)Electronic mail: waltz@fusion.gat.com.

 

In this paper, we test the accuracy of the mQLTA by two-step gyrokinetic simulations: first a linear run to get the quasilinear weight, then second a nonlinear simulation to get the spectral weight as well as the actual nonlinear transport to which the quasilinear transport can be compared in each channel and wave number. The ratio of quasilinear transport to the actual nonlinear transport, which we call the *overage*, is always somewhat larger than one. A key measure of success for the either QLTA are (1) that the overage be nearly the same in each channel (and less importantly in each wave number) and (2) that the overage should be nearly constant across a wide variety of physical case parameters. Note that in theory-based models, the overall average overage is renormed to unity by adjusting a single coefficient on the nonlinear saturation rule for the spectral weight. When a theory-based model fails to match the nonlinear gyrokinetic simulated transport (or the experimental transport for that matter), we do not usually know if there is a failure in the accuracy of the underlying physics (e.g., gyrofluid versus gyrokinetic linear growth rates), the nonlinear saturation rule for the spectral weight, or the quasilinear weight. By using linear and nonlinear gyrokinetics simulations and the actual nonlinearly simulated spectral weight, we can hope to isolate and quantify the success or failure of the mQLTA itself. The main caveat in testing via an initial value time dependent gyrokinetic code is that we can only isolate the leading linear normal mode in each wave number, whereas models such as GLF23 and TGLF (which solve a dispersion matrix and isolate linear normal modes) found it useful to include the first few (at least two) leading normal modes. Since the quasilinear weight of the dominant mode is expected to be larger than that for a subdominant mode, the full spectral weight applied only to the leading mode will tend to produce a larger overage than would be obtained if correctly distributed over both leading and subdominant modes. [At this point we should clarify that by leading and first subdominant "mode" in each wave (toroidal mode) number we typically mean the ion or electron directed "branch" and within each branch mQLTA (as it applied in models) keeps only the most outward "ballooning mode," which is typically the most unstable. There is a continuum of lesser ballooning and less unstable modes with smaller quasilinear weight and lesser but not zero spectral weight. These are left uncounted.]

In contrast with the practical interest in the mQLTA, the fQLTA is mainly of theoretical interest in that it suggests what might be ultimately captured from the quasilinear theory if we could accurately model the frequency spectrum of the spectral weight and in particular that portion not captured by the leading normal mode (or modes) in each wave number. We expect the overages in the fQLTA to be somewhat smaller than those for the mQLTA because the fQLTA does not discount any less unstable "normal modes" or even any "background noise" (i.e., that which cannot be lumped into linear "normal modes"). While expected to have smaller overages, the fQLTA fails to have the required ambipolar particle flows since it involves only the real frequency response function to "external" potential, i.e., there is no feedback of the linear particle motion into a quasineutrality field solve. Since the nearly adiabatic electrons are expected to control the particle transport, we ignore the tracer (fQLTA) ion particle transport.

There is no practical way to test the fQLTA in a direct two-step way, i.e., first finding the linear potential response function over a wide range of frequencies to compute the frequency dependent quasilinear weight and second a nonlinear simulation to capture the frequency dependent spectral weight in each wave number. Instead we develop a one-step test method from nonlinear plasma-linear tracer simulations. The simulations have "plasma" ions and electrons at full densities and identical "tracer" ions and electrons at trace densities. Hence the plasma species alone drive the potential fluctuations and the true (not external or artificial) spectral weight and the tracer species have no feedback on the potential fluctuations. If the tracer species have the nonlinear $E\times B$ as well as linear motion, then the tracer and plasma diffusivities are identical (as we will show). However, if the tracers have only linear motion (by artificially deleting the nonlinear motion), the resulting tracer transport diffusivities can be taken as the fQLTA diffusivities and we can again compute the overages. Aside from that we can also simulate the so-called *passive tracer diffusivity* by retaining both the linear and then nonlinear terms but deleting the linear curvature and parallel motion in the tracer species.

In Sec. II, we formulate both the mQLTA and fQLTA in more mathematical detail. We show that they are actually identical if the frequency spectrum for each normal mode is taken to have a Lorentzian line width (or decorrelation rate) chosen to be the linear growth rate. (This is of course an unphysical choice since modes with the larger growth rates naturally have smaller decorrelation rates.) In Sec. III, we use the GYRO (Ref. 7) gyrokinetic code to demonstrate a quantified success for both the mQLTA and fQLTA in a variety of GA standard cases with kinetic ions and electrons, i.e., constancy of overage across wave number, transport channel, and cases. We also isolate and quantify *nonlinearly induced transport* in linearly stable wave numbers. In Sec. IV, we extend these cases to much larger temperature gradients to quantify a breakdown in mQLTA (and to a lesser extent fQLTA) in the case of (unrealizable) strong particle pinches. Section V demonstrates a surprising breakdown of the mQLTA (but not fQLTA) for the ion temperature gradient (ITG) adiabatic electron case and we speculate on its cause. Section VI briefly provides some overall conclusions. We emphasize that our focus is on testing the quasilinear transport approximation itself (as well as tracer methods) and not on the physical veracity or fidelity of the underlying model, which is here the nonlinear electrostatic, toroidal, and collisionless local gyrokinetic equations. A similar testing program could be carried out with other nonlinear models, e.g., gyrofluid, gyro-Landau-fluid (with dissipative closures), or simple fluid moment models.

## II. FORMULATION OF THE QLTA

The flux surface average ion and electron energy as well as particle fluxes $[Q_i, Q_e, \Gamma]$ and their respective diffusivities $[\chi_i, \chi_e, D_e]$ are given by the local radial and flux surface average (indicated by wave number $k$ summation) as well as

time average (indicated by $\{\cdots\}^t$) correlation of the energy and particle moment fluctuations $[\delta E_{ik}^{(\mathrm{nl})}, \delta E_{ek}^{(\mathrm{nl})}, \delta n_k^{(\mathrm{nl})}]$ with the radial $E\times B$ velocity fluctuations $\delta v_{Ek}^{(\mathrm{nl})}=(c/B)ik_y\delta\phi_k$:

$$[Q_i,Q_e,\Gamma] \equiv [-n_i\chi_i dT_i/dr, -n_e\chi_e dT_e/dr, -D_e dn/dr] \equiv \mathrm{Re}\,\Sigma_k\{[\delta E_{ik}^{*(\mathrm{nl})}, \delta E_{ek}^{*(\mathrm{nl})}, \delta n_k^{*(\mathrm{nl})}]\delta v_{Ek}^{(\mathrm{nl})}\}^t, \quad (1)$$

where the superscript "(nl)" indicate actual fluctuations in a nonlinear simulation. The mQLTA flux in each channel is a wave number $k$ and mode label $m$ convolution of a quasilinear weight and field intensity spectral weight,

$$\text{transport flux} \approx \Sigma_k\Sigma_m\{\text{QL weight}\}_k(m) \otimes \{\text{spectral weight}\}_k(m). \quad (2)$$

For example, the particle flux for a normal mode $m$ is $\Gamma_{km}^{(\mathrm{ql})}\equiv \mathrm{Re}\,\delta n_{km}^*\delta v_{Ekm}$, so the particle flux mode quasilinear weight is

$$\{\text{QL weight}\}_{km} = \mathrm{Re}\{\delta n_{km}^*\delta v_{Exkm}\}/\{\delta\phi_{km}^*\delta\phi_{km}\}, \quad (3)$$

whereas the field intensity spectral weight is taken from a model mixing length saturation rule or, in the case of this paper, a nonlinear simulation:

$$\{\text{spectral weight}\}_{km} = \{\delta\phi_{km}^*\delta\phi_{km}\}, \quad (4)$$

where $\delta n_{km}$ is the normal mode density response to the normal mode potential $\delta\phi_{km}$ perturbation. Since each normal mode used quasineutrality $\delta n_{km}^e=\delta n_{km}^i$ in the field solve, particle flows are automatically ambipolar, i.e., $\Gamma_{ekm}^{(\mathrm{ql})}\equiv\Gamma_{ikm}^{(\mathrm{ql})}$. However, as indicated, the initial value gyrokinetic code can only find the leading mode ($m=1$) and the full spectral weight on the nonlinear simulation can only be placed on the leading mode $\{\delta\phi_k^*(1)\delta\phi_k(1)\}\approx\{\delta\phi_k^{*(\mathrm{nl})}\delta\phi_k^{(\mathrm{nl})}\}^t$, where it would be a more accurate test to write $\{\delta\phi_{km}^*\delta\phi_{km}\}=\{\delta\phi_{km}^{*(\mathrm{nl})}\delta\phi_{km}^{(\mathrm{nl})}\}^t$. Note that GYRO (Ref. 7) has a recently added facility to isolate subdominant linear normal modes like the GENE code,[8] hence it would be straightforward to find the subdominant quasilinear weights. However it would be difficult to separately isolate each $\{\delta\phi_{km}^{*(\mathrm{nl})}\delta\phi_{km}^{(\mathrm{nl})}\}^t$ component.

The fQLTA simply replaces the discreet mode ($m$) summation by a frequency $\omega$ integral appropriate to a time average $\Sigma_m\Rightarrow\int d\omega/2\pi$. For a special form of the frequency spectrum assigned to the spectral weight of a normal mode, the fQLTA and mQLTA are identical as we now demonstrate. The linear density frequency response to a potential $\delta\phi_k(t)=\delta\phi_{k\omega}\exp(-i\omega t)$ is

$$\delta n_{k\omega} = n_0(e/T)\delta\phi_{k\omega}\times\left\{1-\int d\upsilon^3 F_0(E)J_0^2(k\rho)[\omega-\omega_{*k}^\upsilon]/[\omega+i\varepsilon-\varpi_k^\upsilon]\right\}, \quad (5)$$

where $\omega_{*k}^\upsilon=(ck_yT/eB)[L_n^{-1}+(E/T-3/2)L_T^{-1}]$, $\varpi_k^\upsilon=k_\parallel v_\parallel+\omega_D$ with $J_0^2$ as the double gyroaverage, $F_0$ as the energy $E=m\upsilon^2/2$ Maxwellian, and $\omega_D$ as the curvature drift frequency. $L_n^{-1}$ and $L_T^{-1}$ are the inverse density and temperature gradient lengths. Only the nonadiabatic part [second term in Eq. (5)] contributes to transport. The particle flux per wave number as the fQLTA convolution over frequency is

$$\{\delta n_k\delta v_{Ek}^*\}^t = n_0\int_{-\infty}^{\infty}d\omega/2\pi(ck_y/B)(e/T)\times\int d\upsilon^3F_0J_{0k}^2[\delta\phi_{k\omega}^*\delta\phi_{k\omega}]\times\mathrm{Im}\{[\omega-\omega_{*k}^\upsilon]/[\omega+i\varepsilon-\varpi_k^\upsilon]\}. \quad (6)$$

Using $1/[\omega+i\varepsilon-\varpi_k^\upsilon]=P\{1/[\omega-\varpi_k^\upsilon]\}-i\pi\delta(\omega-\varpi_k^\upsilon)$ transport appears to be only at the wave-particle resonance,

$$\{\delta n_k\delta v_{Ek}^*\}^t = (n_0/2)(ck_y/B)(e/T)\int d\upsilon^3F_0J_0^2[\delta\phi_{k\varpi_k^\upsilon}^*\delta\phi_{k\varpi_k^\upsilon}]\times[\varpi_k^\upsilon-\omega_{*k}^\upsilon]. \quad (7)$$

Since the ion and electron resonances would not normally overlap, it would appear that the particle flow is not automatically ambipolar. This is why the fQLTA is usually rejected in model building. However, using a Lorentz line model,

$$[\delta\phi_{k\omega}\delta\phi_{k\omega}^*] = I_{0k}\{2\Delta\omega_k/[(\omega-\omega_{0k}-\delta\omega_k)^2+\Delta\omega_k^2]\}, \quad (8)$$

for a normal mode $m$ and ignoring the nonlinear line shift by taking $\omega_{0k}+\delta\omega_k\Rightarrow\omega_k^m$ to be the linear frequency, and (following the QualiKiz model[6]) taking the mode decorrelation rate to be $\Delta\omega_k\Rightarrow\gamma_k^m$, we find that the fQLTA is identical to the mQLTA. This is clearly an unphysical choice since the weak (or direct) interaction approximation[9,10] has $\Delta\omega_k=-\gamma_k^m+\gamma_k^{(\mathrm{nl})}$ (where $\gamma_k^{(\mathrm{nl})}$ is the nonlinear rate), i.e., more strongly growing modes have smaller, not larger, decorrelation rates. Nevertheless substituting these choices into Eq. (7), the fQLTA takes the form

$$\{\delta n_k\delta v_{Exk}^*\}^t = n_0(ck_y/B)(e/T)\int d\upsilon^3F_0J_{0k}^2\times[\varpi_k^\upsilon-\omega_{*k}^\upsilon]\gamma_k^m/[(\varpi_k^\upsilon-\omega_k^m)^2+\gamma_k^{m2}]I_{0k}. \quad (9)$$

The $\delta\phi_k(t)=\delta\phi_k(m)\exp(-i\omega_k^mt+\gamma_k^mt)$ the mQLTA particle flux is

$$\{\delta n_k\delta v_{Exk}^*\}^t = n_0(ck_y/B)(e/T)\int d\upsilon^3F_0J_{0k}^2\times\mathrm{Im}[\omega_k^m+i\gamma_k^m-\omega_{*k}^\upsilon]\gamma_k^m/[\omega_k^m+i\gamma_k^m-\varpi_k^\upsilon]I_{0k}, \quad (10)$$

where we identified $\delta\phi_{km}\delta\phi_{km}^*\exp(2\gamma_k^mt)$ with $I_{0k}$. The fQLTA form in Eq. (9) is in fact identical to the mQLTA form in Eq. (10). Dividing the right-hand side of Eq. (9) by the spectral weight $I_{0k}$ provides the most transparent form of the particle quasilinear weight (and similarly for the energy channels by inserting an $E$ factor in the velocity integral). At least for weak turbulence $\gamma_{0k}\ll\omega_{0k}$ (which is normally the case for magnetically confined plasma turbulence), it is apparent that subdominant modes with smaller growth rates $\gamma_{0k}$ are expected to have smaller quasilinear weights (as well as smaller spectral weights).

TABLE I. Overages for two-step test of the mQLTA as ratios of quasilinear to nonlinear diffusivities. The parenthetic ratios are the normalized overages (overages divided by the average overage of 1.64).

| | $\chi_i^{(ql)}/\chi_i^{(nl)}$ | $\chi_e^{(ql)}/\chi_e^{(nl)}$ | $D_e^{(ql)}/D_e^{(nl)}$ |
|---|---|---|---|
| ITG/TEM | 17.9/12.1=1.47 (0.87) | 5.83/3.42=1.70 (1.03) | −3.21/−2.01=1.79 (1.09) |
| TEM1 | 21.8/15.0=1.45 (0.88) | 21.0/15.3=1.37 (0.84) | 7.86/5.50=1.42 (0.87) |
| TEM2 | 43.8/25.9=1.69 (1.03) | 56.3/30.3=1.85 (1.12) | 12.2/5.9=2.07 (1.26) |

We refer to the overage in each channel or wave number as the ratios $[\chi_i^{(ql)}/\chi_i^{(nl)}, \chi_e^{(ql)}/\chi_e^{(nl)}, D_e^{(ql)}/D_e^{(nl)}]$. Success of the QLTA will be measured in the constancy of the overage across wave number, channel, and parametric case variation.

## III. STANDARD CASE ILLUSTRATIONS VALIDATING THE QLTA

To test the QLTA, we do linear and nonlinear GYRO (Ref. 7) simulations on the GA-ITG/TEM standard case: $q=2$, $\hat{s}=d\ln q/d\ln r=1$, $R/a=3$, $r/a=1/2$, $T_i/T_e=1$, $n_i/n_e=1$, $a/L_T=3$, $a/L_n=1$, with $\alpha=0$ infinite aspect ratio circular "$s$-$\alpha$" geometry. The unit of length "$a$" is the minor radius ($r$) of the last closed flux surface. For cases with collisionless and electrostatic kinetic electrons, we take $\mu=\sqrt{M_i/m_e}=60$. ITG-ae refers to the ITG adiabatic electron standard case. Diffusivities are in gyro-Bohm units $\chi_{gB}=[c_s/a]\rho_s^2$, where $\rho_s=c_s/\Omega_i$, $c_s=\sqrt{T_e/M_i}$, and $\Omega_i=eB/cM_i$. The ITG mode dominates at low-$k$ and the trapped electron mode leads from $\sim 0.5<k_y\rho_s\leq 1.0$. High-$k$ electron temperature gradient (ETG) modes with $k_y\rho_s>1.0$ (Ref. 11) are not considered. The GA-TEM2 case has similar parameters with $a/L_T=3\Rightarrow 1$ and $a/L_n=1\Rightarrow 3$, which leads to the dominance of the trapped electron mode (TEM) branch at all $k_y\rho_s\leq 1.0$. The GA-TEM1 case with $a/L_T=2$ and $a/L_n=2$ is mixed with the ion (ITG) branch and the electron (TEM) branch having nearly the same growth rates. These GA standard cases have been considered previously.[11–14] Typical numerical parameters for these GYRO simulations are as follows: $[L_x/\rho_s, L_y/\rho_s]=[126,126]$, $\Delta x/\rho_s=0.75$, 16 modes in $0\leq k_y\rho_s\leq 0.75$ with 12 grids in the parallel direction, 15 in the gyroaverage, and 5 in the radial derivative; there are 128 velocity space grids per spatial cell (eight energies, eight pitch angles, and two parallel directions). The statistical average values from the nonlinear simulations were typically taken from time averages starting at $100[a/c_s]$ and lasting to $1000[a/c_s]$.

Table I shows the overages for the two-step linear-nonlinear test of the mQLTA. The *average overage* is 1.64 in Table I, which provides a *normalized overage* with an rms deviation of 13.5%, which has to be considered a successful result. Figure 1 shows the overages across wave numbers as well as the spectral weight for the three cases. It is quite apparent that the overages at higher-$k$ are (sometimes considerably) larger than the net transport overages, but this has little effect on the on the net transport overages since the spectral weight is weak at the high-$k$. The apparent breakdown of the QLTA at higher-$k$ is expected from the "$k^2D$" model of nonlinear wave-particle resonance broadening.[15,16] It is useful to note that the gyrokinetic GENE code has been used to show that the $E\times B$ nonlinearity can be well represented by a (purely real) $k_y^2D$ linear damping for a cold ion TEM case (and furthermore that the "$D$" tracks the variation in $\chi_e$).[17] The large jump in the overages for $k_y\rho_s>0.5$ in the ITG/TEM case can be associated with the transition from the dominance of the ion (ITG) to the electron (TEM) branch at higher-$k$. The ITG/TEM case with its pinched particle flow ($D<0$) seems to have the most tenuous validity for the mQLTA and we return to that in Sec. IV. The overage for the ITG-ae case is $\chi_i^{(ql)}/\chi_i^{(nl)}=6.24/3.76=1.66$, which is very close to the average overage of 1.64 in the ITG/TEM, TEM1, and TEM2 cases of Table I. We return to the ITG-ae case at higher turbulence levels in Sec. V.

Turning to the validation of the ITG/TEM case for the one-step tracer test of the fQLTA, we first verify the plasma-tracer method. Table II shows that, indeed, tracer diffusivities are identical to the plasma tracer diffusivities if the nonlinearity in the tracer species is retained. Table III provides the overages for the fQLTA by deleting the nonlinearity in the

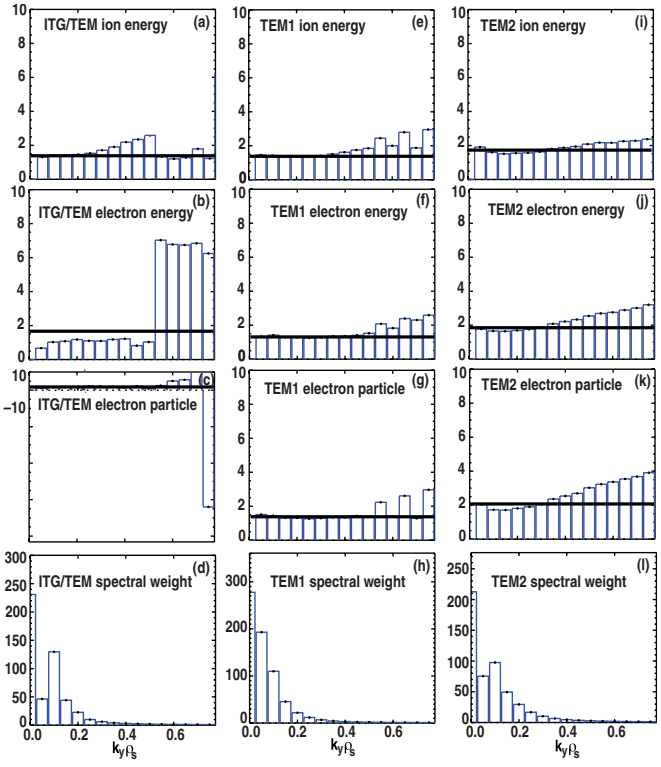


FIG. 1. (Color online) Wave number spectrum of *overage* for ion energy (a) [(e) and (i)], electron energy (b) [(f) and (j)], and particle(c) [(g) and (k)] transport, and spectral weight (d) [(h) and (l)] for ITG/TEM, and (TEM1 and TEM2), respectively. The horizontal lines indicate the net overage in each channel as given in Table I.

TABLE II. Ratio of the tracer diffusivities to plasma diffusivities for the ITG/TEM case. The asterisks denote that some difference in the electron diffusivities might be expected since the "tracer electrons" (and also both plasma and tracer ions) are explicitly evolved whereas the "plasma electrons" have a mixed explicit-implicit (for fast parallel motion) evolution.

| | $\chi_i^{(\mathrm{tr})}/\chi_i^{(\mathrm{nl})}$ | $\chi_e^{(\mathrm{tr})}/\chi_e^{(\mathrm{nl})}$ | $D_i^{(\mathrm{tr})}/D_i^{(\mathrm{nl})}$ | $D_e^{(\mathrm{tr})}/D_e^{(\mathrm{nl})}$ |
|---|---|---|---|---|
| ITG/TEM | 12.0/12.0 | 3.22/3.28* | −2.03/-2.02 | −2.01/−2.0* |

tracer species. As expected the tracer particle flow is not ambipolar with the tracer ion diffusivity about two times larger than the tracer electron diffusivity. Since electron nonadiabaticity controls particle flow, we consider only the electron particle flow overage of 1.43, which is close to the ion energy overage but larger than the electron energy overage, which is rather smaller than expected. It seems reasonable that fQLTA overages would be smaller than those for the mQLTA since the spectral weight is also distributed in part over the subdominant modes, which should have smaller quasilinear weights (as shown in Sec. II).

In passing, we note that the one-step plasma—tracer simulation technique is ripe for numerical experimentation, which may lead to a better understanding of the nature of turbulent plasma transport. We give two examples: first *quasinonlinear transport* (here) and second passive tracer diffusivity (below). We define *quasinonlinear transport* by deleting the linear $E\times B$ drive ("omega-star" term) but retaining the nonlinear $E\times B$ motion in the tracers. (It is in contrast with tracer quasilinear transport, which deletes nonlinear $E\times B$ and retains linear $E\times B$.) In the ITG/TEM case at hand, for the ion energy channel, $\chi_i^{(\mathrm{qnl})}+\chi_i^{(\mathrm{ql})}=-4.83+16.7=11.87\sim 11.3=\chi_i^{(\mathrm{nl})}$ (from Table III), as might be expected (from simple addition). However, for the electron channel, $\chi_e^{(\mathrm{qnl})}+\chi_e^{(\mathrm{ql})}=-1.18+3.66=2.48<3.7=\chi_e^{(\mathrm{nl})}$ and $D_e^{(\mathrm{qnl})}+D_e^{(\mathrm{ql})}=-1.75-2.7=-4.45\ll -1.90=D_e^{(\mathrm{nl})}$ (again from Table III), the expected simple rule does not appear to hold. This is likely because the dominant low-$k$ ITG turbulence is driving most of the electron transport. Indeed it is well understood that an unstable electron mode cannot drive a particle pinch ($D<0$), which must be driven by the unstable ion (ITG) branch.[18]

There is an alternative numerical experiment demonstrating quasinonlinear (or nonlinearly induced) transport: standard plasma species simulations (without tracers) can be made with the linear $E\times B$ drive deleted for a single wave number. There will be no linearly unstable mode in the deleted wave number. However, as illustrated in Fig. 2, some transport will appear in the deleted wave numbers, which can be compared to that in nearby linearly unstable wave numbers. A more physical example of low-$k$ driven, high-$k$ nonlinear transport in ETG stable plasmas has been demonstrated previously.[11]

Alternatively, as a second tracer methods example, we can retain both linear and nonlinear $E\times B$ motion in the tracers while deleting the remaining parallel and curvature drift motions. This could be defined as passive tracer diffusivities $[\chi^{\mathrm{pass\text{-}tr}},D^{\mathrm{pass\text{-}tr}}]$, which can be considerably larger than the actual diffusivities as shown in Table IV. $E\times B$ motion (and only $E\times B$ motion) is independent of mass and charge of the species. This should caution thinking that (for example) experimental trace impurity diffusion can provide any close measure of actual plasma energy or particle diffusion (other than order of magnitude). Scaling the $E\times B$ nonlinear motion (or essentially the transport flows) with the Maxwellian velocity space (energy $\varepsilon$) average $\langle\cdots\rangle^M$ of the linear $E\times B$ motion, it is easy to see that for both ions and electrons

$$\chi^{\mathrm{pass\text{-}tr}}/D^{\mathrm{pass\text{-}tr}}=\frac{L_T\langle\varepsilon[1/L_n+(\varepsilon-3/2)1/L_T\rangle^M}{L_n\langle[1/L_n+(\varepsilon-3/2)1/L_T\rangle^M}=3/2(L_T/L_n+1)\Rightarrow 2, \tag{11}$$

as indicated in Table IV for $[a/L_T,a/L_n]=[3,1]$. If we break up "energy diffusion" into "heat diffusion" and "convective energy diffusion," $Q\equiv nT\chi/L_T\equiv$, $nT(3/2\chi_q/L_T+3/2D/L_n)$, then we find the possibly more familiar and equivalent result $\chi_q^{\mathrm{pass\text{-}tr}}=D^{\mathrm{pass\text{-}tr}}$, i.e., these diffusivities are the same across channel and species.

## IV. EXAMPLE BREAKDOWN OF THE QLTA FOR STRONGLY PINCHED PARTICLE FLOWS

For the practical validity of the QLTA, it is not sufficient for the overage to be constant across wave number and channel, it should also be reasonably constant over a wide variation in case parameters. In Fig. 3 we reconsider the ITG/TEM case over a wide range of temperatures gradients $[2<a/L_{Ti}=a/L_{Te}<9]$, with the overages for mQLTA in Fig. 3(a) and fQLTA in Fig. 3(b). It is apparent that the overages in both energy channels remain nearly constant with that for the fQLTA somewhat lower (about 1.3 versus 1.6) even though the level of energy transport increased four- to eightfold. However overage for the strongly pinched particle flow breaks away considerably from the energy flow: about threefold for the mQLTA and twofold for the fQLTA. In contrast with the fQLTA, the particle mQLTA overage also beaks away with an underflow at $a/L_T=2$. It is tempting to blame the strong breakdown in the particle channel for the mQLTA on the inability to keep subdominant modes. However, in Fig. 4, we show the same scan for the TGLF (Ref. 5) model keeping two leading modes in Fig. 4(a) and only the leading

TABLE III. fQLTA overages as the ratio of the tracer diffusivities to plasma diffusivities for the ITG/TEM case with the tracer nonlinearity deleted.

| | $\chi_i^{(\mathrm{ql})}/\chi_i^{(\mathrm{nl})}$ | $\chi_e^{(\mathrm{ql})}/\chi_e^{(\mathrm{nl})}$ | $D_i^{(\mathrm{ql})}/D_i^{(\mathrm{nl})}$ | $D_e^{(\mathrm{ql})}/D_e^{(\mathrm{nl})}$ |
|---|---|---|---|---|
| ITG/TEM[a] | 16.7/11.3=1.48 | 3.66/3.17=1.15 | −5.1/−1.91 | −2.7/−90=1.43 |

[a]The apparent discrepancy with respect to Table II for the plasma species diffusivities is due to slightly different grids and time averages. The large ion particle diffusivity overage is to be ignored.

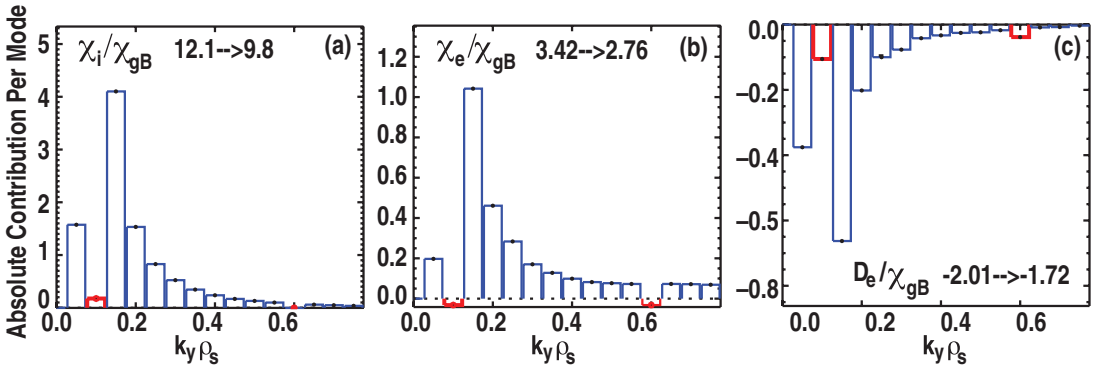


FIG. 2. (Color) ITG/TEM GA-std case ion energy (a), electron energy (b), and particle (c) contribution per mode diffusivity vs wave number with the linear $E\times B$ drive ("omega-star" term) at $k_y\rho_s=0.10$ and $k_y\rho_s=0.60$ deleted hence linearly stable. Purely nonlinearly induced transport is in red. The total transport is somewhat reduced.

mode in Fig. 4(b). Note that the TGLF model normally keeps the two leading modes. The fitted TGLF nonlinear saturation rule for the spectral weight normalizes the average overage to 1.0 as indicated by the red line. The leading mode only scan had the same fitted normalization of the saturation rule for the spectral weight (hence the energy overages fall below 1.0). If one carefully examines the GYRO versus two-mode TGLF particle flow in Fig. 1(b) of Ref. 5, it is readily apparent that there is a scatter about a twofold overage for extreme pinches while normal outflow (down the density gradient) tracks an overage of 1 (as do the energy channels). We can now see that this is due to a clear breakdown of the mQLTA and rather than the fitted saturation rule or the approximate linear gyrofluid model fitted to gyrokinetics.

The breakdown of mQLTA with strong particle pinch is also indicated by comparing the leading mode linear cross-phase angles for the energy and particle channels with the probability distribution function (PDF) contour spectrum of the nonlinear angles as shown in Fig. 5. It is readily apparent that, at lower wave numbers, which contribute the largest transport, the linear density-potential positive (pinched) cross-phase angles break away to more positive from the nonlinear angles at higher turbulence level. In contrast the linear energy-potential negative (normal flow down the gradient) cross-phase angles track the nonlinear angles independent of turbulence level (i.e., $a/L_T=3$ versus $a/L_T=6$). Note that the quasilinear weights are proportional to the cross-phase angles, e.g., from Eq. (3) we have the mQLTA $\{\text{QL weight}\}_{km}=-[ck_y/B][|\delta n_{km}|/|\delta\phi_{km}|]\sin(\vartheta^n_{km})$, where $\vartheta^n_{km}$ is the density cross-phase angle. Just as with the quasilinear weight overage versus wave number (Fig. 1), the linear cross-phase angle is in poor agreement with the nonlinear angle at larger wave numbers in all channels for this ITG/TEM case $a/L_T=3$.

TABLE IV. ITG/TEM GA-std case passive tracer diffusivities compared to actual diffusivities.

| | $\chi_i^{(\text{pass-tr})}/\chi_i^{(\text{nl})}$ | $\chi_e^{(\text{pass-tr})}/\chi_e^{(\text{nl})}$ | $D_i^{(\text{pass-tr})}/D_i^{(\text{nl})}$ | $D_e^{(\text{pass-tr})}/D_e^{(\text{nl})}$ |
|---|---|---|---|---|
| ITG/TEM | 26.3/12.2 | 26.3/3.35 | 13.4/–2.03 | 13.9/–2.03 |

We repeated the ITG/TEM case $a/L_T=3$ mode deletion experiment of Fig. 2 with $a/L_T=9$. The nonlinearly induced transport relative to the linear transport is substantially increased in the pinched particle flow. The QLTA simply cannot capture nonlinearly induced transport.

Note that core particle fueling beams are rather weak in most tokamaks so the typical operating point has a "pinched" by almost "null" point flow in the core with strong outflow (down the density gradient) at the edge to accommodate gas feed and wall recycling. Figure 6 illustrates a similar temperature gradient scan with a (weak ITG modified) TEM2 (strong density gradient $a/L_n=3$ and $a/L_{Te}\geq 1$) case having only normal outflow in the particle channel. Here the mQLTA succeeds in keeping the overages relatively constant. The ITG was kept low to suppress the ITG branch, which in turn makes the ion energy diffusivity large.

## V. MQLTA BREAKDOWN FOR THE SIMPLE ITG-AE CASE

Considering the success of the QLTA for the multichannel kinetic electron cases in Secs. II and III, it was most surprising to find a breakdown of the mQLTA, but not the fQLTA for the simple ITG-ae ion energy flow case going far from threshold to very high turbulence levels. As illustrated in Fig. 7(a), the mQLTA overage increases by 2.1-fold from the overage of 1.64 at the standard point from $a/L_{Ti}=3$ to $a/L_{Ti}=9$, whereas the lower fQLTA overage increases hardly

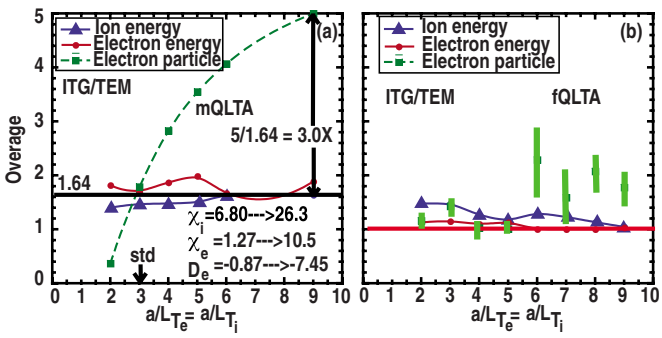


FIG. 3. (Color online) ITG/TEM case *overage* vs temperature gradient for mQLTA (a) and fQLTA (b).

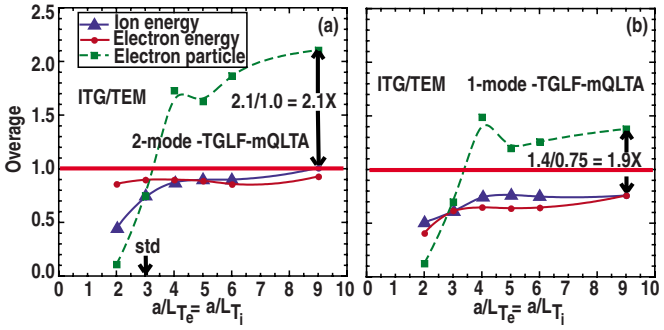


FIG. 4. (Color online) Overage vs temperature gradient for the normal two leading mode TGLF model in (a) and the leading mode only model in (b).

at all. More surprising still is the fact (not shown) that the linear cross-phase angle between pressure and potential perturbations accurately tracks the nonlinear angle. As noted above, the quasilinear weight is dependent on more than the cross-phase angle and we can conclude that the linear ratio in $|\delta p_i|/|\delta\phi|$ is not tracking the nonlinear ratio in the ITGae case. Figure 7(b) shows nearly the same breakdown (1.9-versus 2.1-fold) for the same scan with the leading one-mode (at each wave number) for the TGLF model. (That the TGLF overages are significantly less than one is of no importance since a database of electrostatic kinetic electron GYRO simulations only was used to set the TGLF average overage to one.) It would appear that the breakdown in the mQLTA is not due to the neglect of subdominant linear modes. Figure 7(b) shows that the breakdown is actually

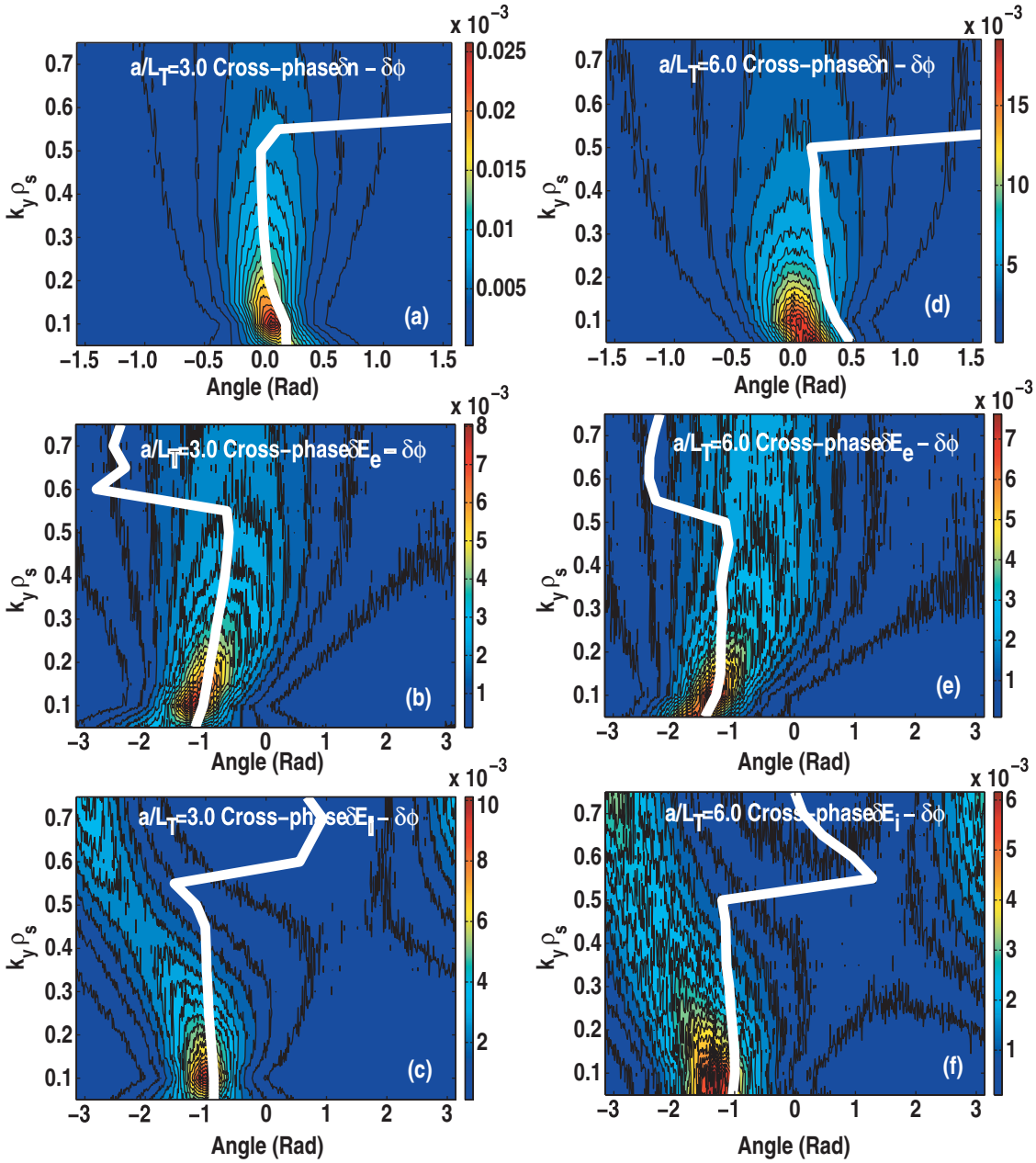


FIG. 5. (Color) Linear (white lines) and nonlinear (PDF contours) cross phase angles vs wave number for particle flow [(a) and (d)], electron energy [(b) and (e)], and ion energy [(c) and (f)] for ITG/TEM case $a/L_T=3$ [(a)–(c)] and $a/L_T=6$ [(d)–(f)] from Fig. 3 $a/L_T$ scan.

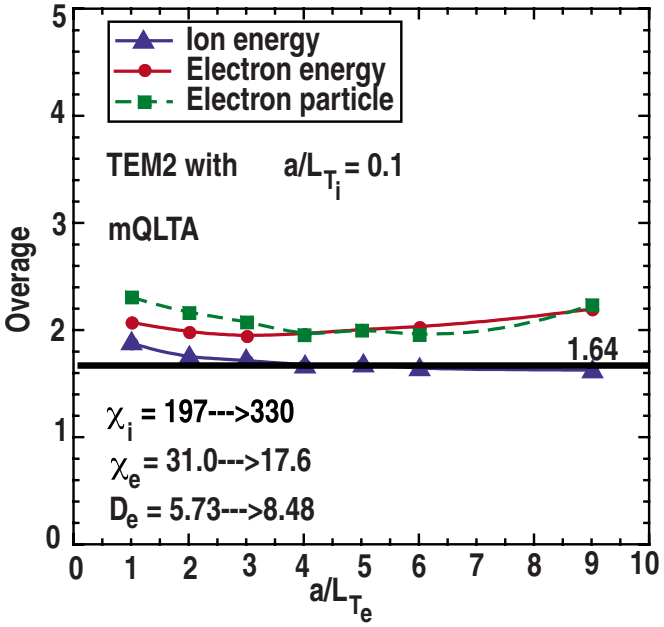


FIG. 6. (Color online) mQLTA *overage* vs temperature gradient for a modified TEM2 case.

slightly worse retaining the TGLF normal leading two-modes (or even four-modes). We can now see that the breakdown in the TGLF model for the ITG-ae case is due to a breakdown in the mQLTA and not the mixing rule for nonlinear saturation of the inaccuracy or the gyrofluid model fits to linear gyrokinetics.

In principle it should make no difference which fields or combination of fluid moments is used to normalize the quasilinear weights and specify the spectral weight, as long they are the same for each wave number (and each transport channel). In Sec. II, Eqs. (3) and (4), respectively (and throughout the paper), we used the potential intensity $|\delta\phi|^2$ as the *norm*, i.e., the phi-norm. However, in model building, it may prove easier to find a good mixing rule for one norm rather than another. The TGLF (Ref. 5) model uses the "*V*-norm" composed of all the even and odd velocity moments of the nonadiabatic distribution function "$\delta g$" from all trapped, passing, ion, and electron species: $\delta f = -[Ze\delta\phi/T]F_0 + \delta g$. This is a natural choice since only the nonadiabatic part of the distribution function contributes to transport and there is a symmetry between $\delta g$ and $\delta\phi$ in the gyrokinetic equation and balance between the time derivative and the nonlinear $E\times B$ motion used to construct the saturation rule. The symmetry suggests that $|\delta V|^2$ and $|\delta\phi|^2$ should equally satisfy the same saturation rule, but in construction of TGLF the *V*-norm proved superior. Figure 7(b) shows the ratio of $|\delta V|^2/|\delta\phi|^2$ normed to one at $a/L_{Ti}=3$. The ratio is nearly constant above $a/L_{Ti}=3$ indicating no distinction between the *V*-norm and phi-norm. However, comparing the smaller variation in overage of the phi-norm mQLTA [red line in Fig. 7(a)] with the overage of the one-mode *V*-norm TGLF [red line in Fig. 7(b)] it would appear that the phi-norm is better in this particular ITGae case.

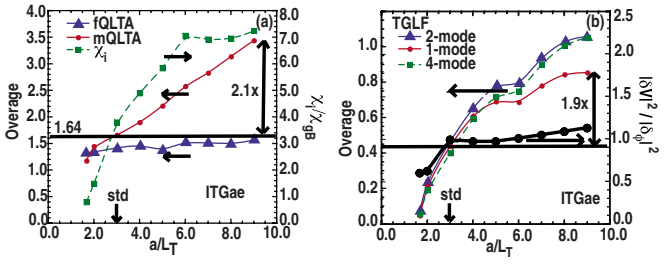


FIG. 7. (Color online) ITGae case overage vs temperature gradient for the fQLTA and mQLTA in (a) and the TGLF model in (b). The simulated $\chi_i/\chi_{gB}$ (green) to right in (a) and fQLTA (blue) and mQLTA (red) overage to left in (a). The two-(blue), one-(red), and four-(green) mode TGLF overages to the left in (b) with ratio of *V*-norm to phi-norm to the right.

Here we speculate as to why the mQLTA (for both the gyrokinetics test and the TGLF model) breaks down but the fQLTA does not breakdown for ITGae. Toroidicity is very strong for ITGae. Even when more than one leading mode is retained in the TGLF model [Fig. 7(b)], the leading and "subdominant" modes are assumed to be centered at the most outward ballooning normal mode $\theta=\theta_0=0$. In fact, there are other normally less unstable modes at larger ballooning angles in the nonlinear simulations ($k_x=k_y\hat{s}\theta_0$). As we have explained earlier, the neglect of these less ballooning and less unstable modes can account (in part) for the overage being larger than 1.0. A more accurate application of the mQLTA should include a convolution over the $\theta_0$-spectrum in Eq. (2).

$$\text{Transport flux(all } \theta_0) \approx \Sigma_k \Sigma_m \sum\nolimits_{\theta_0} \{\text{QL weight}\}_k(m,\theta_0) \otimes \{\text{spectral weight}\}_k(m,\theta_0). \quad (12)$$

In fact, we have been testing a deprecated leading (branch) mode only form of mQLTA,

$$\text{transport flux}(m=1, \quad \theta_0=\theta_0^*) \approx \Sigma_k\{\text{QL weight}\}_k(1,\theta_0^*) \otimes \left[\Sigma_m \sum\nolimits_{\theta_0} \{\text{spectral weight}\}_k(m,\theta_0)\right], \quad (13)$$

where only the spectral weight from the nonlinear simulation is summed over $m$ and $\theta_0$ and $\theta_0^*$ is the $\theta_0$ of the leading mode (normally 0). [With considerably more effort, it is actually possible to do a GYRO test of the more exact mQLTA of Eq. (12) and improved versions of TGLF may use the Eq. (12) form rather than Eq. (2). Note that the fQLTA tracer test needs no such correction.] Since both the quasilinear weight and the spectral weight are roughly proportional to the mode growth rate $\gamma_k(\theta_0)$, we can write a *correction factor* on the overage at each wave number:

$$\{\text{transport flux(all } \theta_0)/\text{transport flux}(m=1, \quad \theta_0=\theta_0^*)\}_k \approx \sum\nolimits_{\theta_0}[\gamma_k(\theta_0)/\gamma_k(\theta_0^*)]^2 \Big/ \sum\nolimits_{\theta_0}[\gamma_k(\theta_0)/\gamma_k(\theta_0^*)]. \quad (14)$$

If the $\theta_0$-spectral shape for $\gamma_k(\theta_0)/\gamma_k(\theta_0^*)$ is unchanged in shape as $a/L_{Ti}$ increases, the overage correction factor will be less than 1.0, but this will not account for the increase in the mQLTA overage seen in Fig. 7(a). However, if at lower $a/L_{Ti}$ the maximum $\gamma_k(\theta_0)/\gamma_k(\theta_0^*)$ is farther away from

$\theta_0 = \theta_0^*$, or if the $\theta_0$-spectrum goes from extremely broad to extremely narrow as $a/L_{Ti}$ increases, then the correction factor will decrease and possibly compensate for the increase in overage seen in Fig. 7(a).

## VI. CONCLUSIONS

We carefully defined and distinguished the practical quasilinear transport approximation mQLTA from the fQLTA of more theoretical interest. Both QLTA involve a wave number ($k$) convolution of a quasilinear weight and a spectral weight. mQLTA has a further convolution of the linear normal mode ($m$) spectrum at each $k$ and the fQLTA has a convolution over frequency ($\omega$) at each $k$. In each case the quasilinear transport in the particle, electron, and ion energy channels was calculated from the nonlinear spectral weight of an actual gyrokinetic simulation. The quasilinear weight for the mQLTA was taken from a linear gyrokinetic run for the leading mode only at each $k$ and for the fQLTA from the gyrokinetic linear (frequency) response at each $k$. Defining the overage as the ratio of the quasilinear diffusivity to the nonlinear transport, a successful QLTA has a nearly constant overage (somewhat larger than 1.0) across wave numbers and most importantly across transport channel in a wide variety of physical case parameters.

Apart from the known lack of ambipolarity, we found the fQLTA to have an amazingly small variation in the overage across channel and across a wide variety of physical case parameters (with and without kinetic electrons). There is a breakaway in the particle transport overage twofold larger than the ion and electron energy overages for a temperature gradient scan in the exceptional case of a very strong particle pinch. In the best cases the fQLTA overages (1.2–1.4) are smaller than mQLTA overages (1.4–1.8) as expected. The mQLTA particle transport overage breakaway for pinched plasma flow are somewhat worse than for the fQLTA and, surprisingly, the mQLTA ion energy transport overage increases strongly with temperature gradient for the simpler ITGae case. Because the fQLTA has no similar breakdown, we speculated that the latter ITGae breakdown might be avoided if (with considerably more effort) mQLTA carried an additional convolution over all ballooning modes rather than taking the quasilinear weight only from the most unstable (and usually most outward) ballooning mode (as in all the tests of mQLTA here). The largest known deviations of the TGLF (Ref. 5) model from fitting the GYRO (Ref. 7) nonlinear gyrokinetic transport simulations appear to track the breakdowns in the mQLTA, i.e., the TGLF deviations appear to result from a breakdown in the quasilinear transport approximation (as applied) and not to a poorly fitted nonlinear saturation rule for the spectral weight or inaccuracy in the gyrofluid versus gyrokinetic equations.

## ACKNOWLEDGMENTS

This work was supported by the U.S. Department of Energy under Grant No. DE-FG02-95ER54309. This work, supported by the European Communities under the contract of Association between EURATOM and CEA, was carried out within the framework of the European Fusion Development Agreement. The views and opinions expressed herein do not necessarily reflect those of the European Commission.

[1] J. Weiland, *Collective Modes in Inhomogeneous Plasma: Kinetic and Advanced Fluid Theory* (Institute of Physics, Bristol, 2000), p. 45.
[2] A. Yoshizawa, S.-I. Itoh, and K. Itoh, *Plasma and Fluid Turbulence: Theory and Modeling* (Institute of Physics, Bristol, 2003), p. 269.
[3] J. E. Kinsey and G. Bateman, Phys. Plasmas **3**, 3344 (1996).
[4] R. E. Waltz, G. M. Staebler, G. W. Hammett, M. Kotschenreuther, and J. A. Konings, Phys. Plasmas **4**, 2482 (1997).
[5] J. E. Kinsey, G. M. Staebler, and R. E. Waltz, Phys. Plasmas **15**, 055908 (2008).
[6] C. Bourdelle, X. Garbet, F. Imbeaux, A. Casati, N. Dubuit, R. Guirlet, and T. Parisot, Phys. Plasmas **14**, 112501 (2007).
[7] J. Candy and R. E. Waltz, J. Comput. Phys. **186**, 545 (2003); see also Phys. Rev. Lett. **91**, 045001 (2003) and the GYRO website http://fusion.gat.com/theory/gyro.
[8] M. Kammerer, F. Merz, and F. Jenko, Phys. Plasmas **15**, 052102 (2008).
[9] B. B. Kadomstev, *Plasma Turbulence* (Academic, London, 1965).
[10] R. E. Waltz, Phys. Fluids **26**, 169 (1983).
[11] R. E. Waltz, J. Candy, and M. Fahey, Phys. Plasmas **14**, 056116 (2007).
[12] J. E. Kinsey, R. E. Waltz, and J. Candy, Phys. Plasmas **12**, 062302 (2005).
[13] J. E. Kinsey, R. E. Waltz, and J. Candy, Phys. Plasmas **13**, 022305 (2006).
[14] R. E. Waltz and C. Holland, Phys. Plasmas **15**, 122503 (2008).
[15] T. H. Dupree, Phys. Fluids **11**, 2680 (1968).
[16] R. E. Waltz and R. R. Dominguez, Phys. Fluids **26**, 3338 (1983).
[17] F. Merz and F. Jenko, Phys. Rev. Lett. **100**, 035005 (2008).
[18] T. Antonsen, B. Coppi, and R. Englade, Nucl. Fusion **19**, 641 (1979); see also B. Coppi and C. Spight, Phys Rev. Lett. **41**, 551 (1978).